Scheme IV

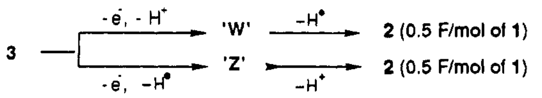

rafluoroborate (TEABF$_4$, supporting electrolyte) was purchased from Aldrich (>99%) and used after vacuum drying (~2 mmHg) at 120 °C for ~30 h. Commercially available Ag/AgCl (from Bioanalytical Systems) was used as reference electrode. HPLC-grade CH$_2$Cl$_2$ (distilled from CaH$_2$) was used for preparative electrolyses.

Spectral Instruments. For spectral measurements, the following instruments have been used: Nicolet 5ZDX FT-IR spectrometer; Perkin-Elmer Lambda 5 UV–vis spectrometer; Brukner WP200SY NMR spectrometer, and Finnigan 4020 Quadrapole or V.G. Model 7035 mass spectrometers.

Electrochemistry. For electrochemical measurements, a Princeton Applied Research (PAR) potentiostat Model 173, a PAR Universal Programmer Model 175, and Yokogawa XY-recorder Model 3036 were employed. A glass cylinder closed at one end, containing 1–5 mM substrate in 5–10 mL of solution, was used for cyclic voltammetry, employing a Pt button (3 × 10^{-3} cm^2) working electrode, surrounded by Pt net cylinder auxiliary electrode. All potentials were measured vs Ag/AgCl reference electrode. An H-type three-compartment cell equipped with medium glass frit as a membrane was used for preparative electrolysis. A polished silver wire quasi-reference electrode, immersed in a glass cylinder with fine glass frit at its end and containing electrolyte solution, was used in these experiments. Typically, the anodic compartment contains 0.3–1 mmmol of ketene imine dissolved in 30 mL of CH$_2$Cl$_2$–0.1 M Et$_4$NBF$_4$. The mixture was stored over molecular sieves (4 Å) which were previously heated to 150 °C under vacuum for ~30 h. All experiments were performed under nitrogen atmosphere free of oxygen (V^{2+}/Zn-Hg trap) and free of moisture (dry molecular sieve trap). Electrolyses were terminated when no ketene imine was detected by TLC. The workup involved stripping of the solvent followed by water addition and extraction into diethyl ether (in which TEABF$_4$ electrolyte is insoluble). After phase separation, drying over MgSO$_4$ and filtration, the solution was concentrated and column separated by Chromatotron (Harrison) Model 7924T, using 2-mm-thick silica gel (PF-254 with CaSO$_4$, from Merck) round plates. Products were separated by gradual elution with 80/20 PE/CH$_2$Cl$_2$ to pure CH$_2$Cl$_2$.

Acknowledgment. The authors are thankful to Dr. S. Cohen from the Hebrew University, Jerusalem, for carrying out X-ray structure measurements and for his valuable assistance in their characterization.

Registry No. **1a**, 14181-84-1; **1b**, 5110-45-2; **1c**, 40012-82-6; **1d**, 29376-76-9; **2a**, 130716-04-0; **29**·C$_6$H$_{14}$, 141344-84-5; **2b**, 130716-05-1; **2c**, 130716-06-2; **2d**, 130716-07-3; **3a**, 130716-08-4; **3b**, 85857-81-4; **3c**, 130716-09-5; **3d**, 130716-10-8; **4a**, 141344-81-2; **4b**, 141344-83-4; **4c**, 141344-77-6; **4d**, 141344-79-8.

Supplementary Material Available: Chemical yields of products from anodic oxidation of **1a**–**1d**, under different drying conditions (Table I), IR and UV–vis data of products (Table IV), and the corresponding crystal data (bond angles, bond lengths, positional and thermal parameters, etc.) of **2b** and **3d** (59 pages). This material is contained in many libraries on microfiche, immediately follows this article in the microfilm version of the journal, and can be ordered from ACS; see any current masthead page for ordering information.

---

(13) Staudinger, H.; Hauser, E. *Helv. Chim. Acta* **1921**, *4*, 887. Barker, M. W.; Perumal, S. I. *Tetrahedron Lett.* **1976**, 349. Kagen, H.; Lillien, I. *J. Org. Chem.* **1966**, *31*, 3728. Crandall, J. K.; Crawley, L. C. *J. Org. Chem.* **1974**, *39*, 489. Barker, M. W.; Sung, H.-S. *J. Heterocycl. Chem.* **1976**, *13*, 1351; 1977, *14*, 693.

(14) Stevens, C. L.; Singhal, G. H. *J. Org. Chem.* **1964**, *29*, 34–37. Stevens, C. L.; French, J. C. *J. Am. Chem. Soc.* **1953**, *75*, 657.

Theoretical Studies on the Prototropic Tautomerism, Structure, and Features of Acridine and 9-Acridinamine Free Bases and Their Protonated Forms

Janusz Rak and Jerzy Błażejowski*

Department of Chemistry, University of Gdańsk,
80-952 Gdańsk, Poland

Randy J. Zauhar

Biotechnology Institute, The Pennsylvania State University,
519 Wartik Laboratory, University Park,
Pennsylvania 16802

Received October 28, 1991

Introduction

Acridine (Acr) and 9-acridinamine (9-AA) are among the simplest representatives of the family of nitrogen heterocyclic bases.[1,2] Many of their features have been investigated employing infrared spectroscopy,[3-6] electronic absorption,[3,7-12] and emission spectroscopies,[11,13-16] NMR spectroscopy,[17] and polarographic[18-21] and dipole moment measurements,[21] as well as theoretical methods.[22-25]

There have long been discussions as to whether 9-AA[3,4,6-8,21,26] and its monoprotonated form[10,27,28] exist in one

---

(1) Albert, A. *The Acridines*, 2nd ed.; Edward Arnold Ltd.: London, 1966.

(2) Acheson, R. M. *Acridines*, 2nd ed.; Interscience: New York, 1973.

(3) Karyakin, A. V.; Grigorovskii, A. M.; Yaroslavskii, N. G. *Dokl. Akad. Nauk. SSSR* **1949**, *67*, 679.

(4) Karyakin, A. V.; Shabya, A. V. *Dokl. Akad. Nauk SSSR, Ser. Khim.* **1957**, *116*, 969.

(5) Sheinker, Yu. N.; Peresteni, E. M. *Dokl. Akad. Nauk SSSR, Ser. Khim.* **1960**, *131*, 1366.

(6) Bacon, N.; Boulton, A. J.; Brownlee, R. T. C.; Katritzky, A. R.; Topsom, R. D. *J. Chem. Soc.* **1965**, 5230.

(7) Acheson, R. M.; Burstall, M. L.; Jefford, C. W.; Sansom, B. F. *J. Chem. Soc.* **1954**, 3742.

(8) Sukhomlina, A. K. *Zh. Obshch. Khim.* **1958**, *28*, 1038.

(9) Zanker, V.; Reichel, A. *Adv. Mol. Spectrosc.* **1960**, *2*, 596.

(10) Capomacchia, A. C.; Schulman, S. G. *J. Pharm. Sci.* **1975**, *64*, 1256.

(11) Kubota, Y.; Motoda, Y. *J. Phys. Chem.* **1980**, *84*, 2855.

(12) Diverdi, L. A.; Topp, M. R. *J. Phys. Chem.* **1984**, *88*, 3447.

(13) Duportail, G.; Mauss, Y.; Chambron, J. *J. Biopolymers* **1977**, *16*, 1397.

(14) Kasama, K.; Kikuchi, K.; Uji-Ie, K.; Yamamoto, S.-A.; Kokobun, H. *J. Phys. Chem.* **1982**, *86*, 4733.

(15) Pant, D. D.; Joshi, G. C.; Triputhi, H. B. *Pramana* **1986**, *27*, 161.

(16) Oelkrug, D.; Uhl, S.; Wilkinson, F.; Willsher, C. J. *J. Phys. Chem.* **1989**, *93*, 4551.

(17) Kokko, J. P.; Goldstein, J. H. *Spectrochim. Acta* **1963**, *19*, 1119.

(18) Chodkowski, J.; Kiwak, W. *Rocz. Chem.* **1974**, *48*, 1401.

(19) Beilis, Yu. I.; Chupakhin, O. N.; Rusinov, V. L.; Bezuglyi, V. D. *Zh. Obshch. Khim.* **1975**, *45*, 606.

(20) Bezuglyi, V. D.; Shapovalov, V. A.; Zhukova, T. N. *Zh. Obshch. Khim.* **1978**, *48*, 2748.

(21) Pushkareva, Z. V.; Kokoshko, Z. Yu. *Dokl. Akad. Nauk SSSR* **1953**, *93*, 77.

(22) Nishimoto, K.; Nakatsukasa, K.; Fujishiro, R. *Theor. Chim. Acta* **1969**, *14*, 80.

(23) Bodor, N.; Dewar, M. J. S.; Harget, A. J. *J. Am. Chem. Soc.* **1970**, *92*, 2929.

(24) Kakitani, T.; Kakitani, H. *Theor. Chim. Acta* **1977**, *46*, 259.

(25) Ni, Y.; Kearns, D. R. *J. Phys. Chem.* **1989**, *93*, 6622.

Chart I

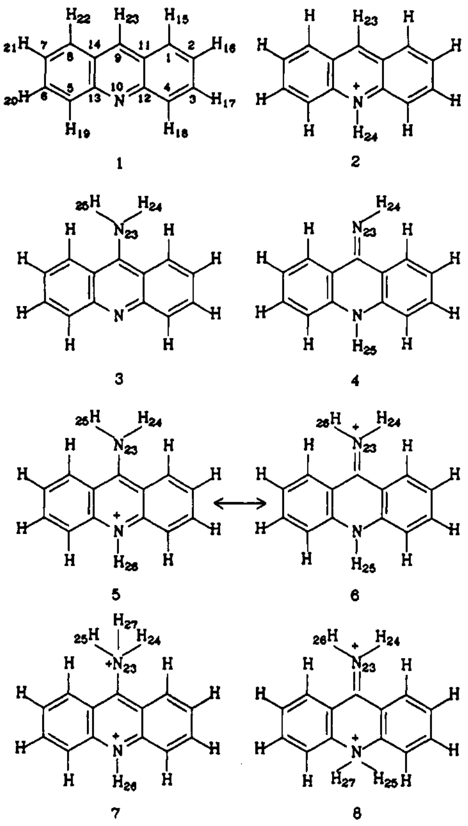

or two tautomeric forms, i.e., amino (**3** and **5**) and imino (**4** and **6**). While some authors supported this idea,[3,4,7,10,27] others did not recognize it.[5,8,17,21,26] Usually the canonic structure of 9-AA has been presented as the amino tautomer **3**.[15,25] The two forms arise from prototropic tautomerism characteristic of 9-AA derivatives.[29-31]

The only report on the crystal structure of 9-AA hemihydrate reveals that the molecule occurs as an amino tautomer.[32] In the crystal structures of mono- and dihydrates of the hydrochloride, protonation takes place at the endocyclic nitrogen.[33,34] Such form, however, can well be created either by the proton attachment to N_{10} of the amino tautomer **3** or by the protonation at N_{23} of the imino form **4**. In consequence one obtains two mesomeric structures **5** and **6**, respectively, which characterize the identical arrangement of atoms in the molecule. To shed more light on structural features of molecules in various forms, as well as their thermodynamic and physicochemical properties, we have employed the AM1 quantum chemistry method.[35]

9-AA is a molecule of biological relevance.[1,2] This results from its distinctive mutagenic activity[36-38] and interaction with DNA[11-13,39] and other biologically important molecules.[11,40] Many experimental[39] and theoretical[38-41] efforts have therefore been undertaken to explain the nature of these interactions. To show sites of potential specific interactions and facilitate insight into the origin of these intermolecular interactions[27,42] we calculated electrostatic potential maps.

Methods

MO Calculations. Molecular orbital calculations have proved useful in investigations of tautomeric phenomena.[43-45] The systems investigated were too large to complete advanced ab initio calculations; hence, we have chosen the semiempirical AM1 method which has recently been used most frequently when examining structure, energetics, and properties of various tautomeric forms.[44-48] It also correctly reproduced tautomeric equilibria in several systems.[44-46,49,50]

The molecules were modeled using SYBYL molecular modeling software, version 5.2 (provided by TRIPOS Associated, Inc.). These structures were then optimized by the semiempirical AM1 method[35] (incorporated in the MOPAC, version 4.0[51]) provided with BFGS energy minimization procedure (all calculations were done in the "precise" option, gradients always being less than 0.4). The geometries and energies of molecules in the transition state for the rotation or inversion were studied combining the following three procedures: *saddle point* geometry estimation,[53] gradient minimization in the saddle point (NLLSQ),[51] and evaluation of the force constants.[51] This always afforded a single negative frequency for the molecule in the transition state. The MOPAC routines were used to evaluate heats of formation, entropies, dipole moments, and energies of HOMO and LUMO orbitals of molecules (the thermochemical quantities refer to 298 K).

Molecular Electrostatic Potential (MEP). MEP (V_i) at a given site i around the molecule was evaluated on the basis of the approximate formula

$$V_i = \sum_{j=1}^{n} \frac{q_j}{r_{ij}} \qquad (1)$$

where q_j represents net charge at atom j, r_{ij} is the distance between atom j and site i, and n denotes the number of atoms in the molecule.[54,55] If at site i point charge q_i is present, the energy

---

(26) Short, L. N. *J. Chem. Soc.* **1952**, 4584.

(27) Capomacchia, A. C.; Casper, J.; Schulman, S. G. *J. Pharm. Sci.* **1974**, *63*, 1272.

(28) Singh, P.; Gupta, S. P. *J. Pharm. Sci.* **1978**, *67*, 706.

(29) Stezowski, J. J.; Kollat, P.; Bogucka-Ledochowska, M.; Glusker, J. P. *J. Am. Chem. Soc.* **1985**, *107*, 2067.

(30) Galy, J.-P.; Faure, R.; Barbe, J.; Elgurero, J. *Spectrosc. Lett.* **1988**, *21*, 809.

(31) Rak, J.; Blazejowski, J.; Nowaczyk, K.; Kawski, A. *J. Fluorescence* **1991**, *1*, 57.

(32) Chaudhuri, S. *J. Chem. Soc., Chem. Commun.* **1983**, 1242.

(33) Talacki, R.; Carrell, H. L.; Glusker, J. P. *Acta Crystallogr., Sect. B* **1974**, *30*, 1044.

(34) Courseille, C.; Geoffre, S.; Busetta, B. *Cryst. Struct. Commun.* **1980**, *9*, 287.

(35) Dewar, M. J. S.; Zoebisch, E. G.; Healy, E. F.; Stewart, J. J. P. *J. Am. Chem. Soc.* **1985**, *107*, 3902.

(36) Lerman, L. S. *J. Mol. Biol.* **1961**, *3*, 18.

(37) Orgel, A.; Brenner, S. *J. Mol. Biol.* **1961**, *3*, 762.

(38) Pullman, B. *Compt. Rend.* **1962**, *255*, 3255.

(39) Wirth, M.; Buchardt, O.; Koch, T.; Nielsen, P. E.; Norden, B. *J. Am. Chem. Soc.* **1988**, *110*, 932.

(40) Nuss, M. E.; Marsh, F. J.; Kollman, P. A. *J. Am. Chem. Soc.* **1979**, *101*, 825.

(41) Cieplak, P.; Rao, S. N.; Grootenhuis, P. D. J.; Kollman, P. A. *Biopolymers* **1990**, *29*, 717.

(42) Hadzi, D.; Koller, J.; Hodoscek, M.; Kocjan, D. In *Modeling of Structure and Properties of Molecules*, Maksic, Z. B., Ed.; Ellis Harwood Ltd.: London, 1987; p 286.

(43) Kwiatkowski, J. S.; Zielinski, T. J.; Rein, R. *Adv. Quantum Chem.* **1986**, *18*, 85.

(44) Fabian, W. M. F. *J. Phys. Org. Chem.* **1990**, *3*, 332.

(45) Les, A.; Adamowicz, L. *J. Phys. Chem.* **1990**, *94*, 7201.

(46) Karelson, M. M.; Katritzky, A. R.; Szafran, M.; Zerner, M. C. *J. Org. Chem.* **1989**, *54*, 6030.

(47) Eberlin, M. N.; Takahata, Y.; Kascheres, C. *THEOCHEM* **1990**, *66*, 143.

(48) Buemi, G. *J. Chem. Soc., Faraday Trans.* **1990**, *86*, 2813.

(49) Katritzky, A. R.; Karelson, M. M. *J. Am. Chem. Soc.* **1991**, *113*, 1561.

(50) Worth, G. A.; King, P. M.; Richards, W. G. *Biochim. Biophys. Acta* **1989**, *993*, 134.

(51) Stewart, J. J. P. *J. Comput.-Aided Mol. Design* **1990**, *4*, 1.

(52) Shanno, D. F. *J. Optim. Theor. Appl.* **1985**, *46*, 87.

(53) Dewar, M. J. S.; Healy, E. F.; Stewart, J. J. P. *J. Chem. Soc., Faraday Trans 2* **1984**, *80*, 227.

(54) Upton, R.; Gasking, H. *Int. Lab.* **1988**, *9*, 24.

Table I. Physicochemical Characteristics of Acridine, 9-Acridinamine, and Their Protonated Forms

compd no.	physicochemical charact: heat of formation (ΔH_f) (kcal/mol): calcd	lit.	proton affinity (PA) (kcal/mol): calcd	lit.	entropy (*S*) (cal/(mol K))	dipole moment (DM) (D): calcd	lit.	energy (eV): LUMO	HOMO
9	77.177	69.9[a]	228.9	233.2[h]	94.629	1.845	1.95[i] 2.09[j] 2.15[k] 2.29[l]	−1.043	−8.575
10	215.472	203.8[b]			95.356			−5.472	−12.922
11	76.011	66.0[c]	240.6[d] 208.4[d]		102.273	3.306	4.14[m]	−0.802	−7.986
12	76.377		241.0[e] 206.5[e]		101.238	3.041		−0.246	−8.272
13	202.579		113.5[f] 112.9[g]		104.374			−5.115	−12.352
14	234.860				103.308			−5.121	−12.311
15	237.103				100.552			−4.477	−13.473
16	456.862				104.021			−9.807	−16.517
17	456.266				101.414			−9.454	−17.435

[a] Reference 56. [b] References 57 and 58. [c] Estimated taking the value of ΔH_f for the crystalline 9-acridinamine from ref 59 (equal to 38.0 kcal/mol) and adding enthalpy of sublimation (ΔH_s) of the compound determined by the thermogravimetric method (analogously as described in ref 57; ΔH_s = ca. 28 kcal/mol. [d] First value corresponds to the reaction 13 → 11 + H^+, and the second one describes the process 14 → 11 + H^+. [e] First value corresponds to the reaction 13 → 12 + H^+, whereas the second one describes the process 15 → 12 + H^+. [f] Value corresponding to the reaction 17 → 13 + H^+. [g] Value corresponding to the reaction 16 → 13 + H^+. [h] Reference 58. [i] References 21 and 60. [j] Reference 61. [k] Reference 62. [l] Reference 63. [m] References 21 and 26.

Table II. Calculated Geometric Parameters (Bond Lengths in Å, Angles in deg)

compound	bond length: C_9–N_{23}	N_{10}–C_{12}	bond order: C_9–N_{23}	N_{10}–C_{12}	dihedral angle: C_{11}–C_9–C_{14}–C_{13}	C_{12}–N_{10}–C_{13}–C_{14}	C_{11}–C_9–N_{23}–H_{24}
9		1.355		1.388	0.12	0.12	
10		1.377		1.191	0.00	0.00	
11	1.378	1.353	1.159	1.373	−0.84	0.42	17.05
12	1.292	1.394	1.891	1.071	−17.92	17.97	−0.67
13	1.345	1.380	1.378	1.138	−0.05	0.00	0.00
14	1.463	1.351	0.932	1.395	−2.33	0.61	30.03
15	1.284	1.468	1.942	0.924	−29.66	33.73	−0.35
16	1.467	1.371	0.949	1.232	−2.55	0.79	29.73
17	1.321	1.468	1.603	0.927	−23.50	28.65	−0.80

of electrostatic interaction between this charge and a molecule is equal to q_iV_i. For V_i calculations net atomic charges for the lowest energy structures were used. We show, first, the surfaces corresponding to an electrostatic interaction energy of ±0.5 kcal/mol with a unit positive test charge (3-D maps of MEP) and, second, points at constant values of electrostatic interaction energy ($|E_i|$) with a trial unit point charge (2-D maps of MEP).

Results and Discussion

Structural Features. The set of two primarily designed structures for the amino tautomer, with planar and perpendicular arrangement of the $-NH_2$ group to the acridine, and four structures for the neutral imino form of 9-AA, with various possible arrangements of the H_{25} and $=N_{23}H_{24}$ fragments relative to the acridine skeleton, was reduced by AM1 to two, one for each tautomer (11 and 12, respectively), exhibiting the lowest energy (Table I). 9-AA has two protonation sites. Thus, attaching a proton to 11 and 12 one obtains four different primary structures. The AM1 method reduced the amino form monoprotonated at N_{10} and imino form monoprotonated at N_{23} to one structure (13) which characterizes the lowest energy. This structure can be considered as a superposition of two mesomeric forms (5 and 6) which exhibit the same arrangements of atoms in the molecule. Two other structures, 14 and 15, which originate from 11 and 12 have much higher energy. Two structures, one for each tautomer, were designed for doubly protonated 9-AA. Their optimization led to 16 and 17 which exhibit comparable energies.

The AM1 method predicts a completely planar structure for the lowest energy monoprotonated 9-AA (13) (Table II). The acridine moiety is also planar in the amino tautomer of 9-AA 11, as in neutral and protonated acridine (9 and 10). Slight deviation from planarity is only expected in amino structures 14 and 16. On the other hand, in all imino structures (12, 15 and 17) the central ring is folded along the $C_9 \cdots N_{10}$ axis, and thus the whole skeleton is nonplanar. The occurrence of such unplanarity has been confirmed by X-ray investigations of 9-AA derivatives which crystallize in the imino form.[29,64] In these imino forms (12, 15, and 17) the $=NH$ or $=NH_2^+$ groups are directed away from the concave side of the acridine nucleus; the H atom at N_{10} in 12 lies almost on the line connecting C_9 and N_{10}, and five atoms in 17, i.e., C_9, N_{10},

---

(55) Liwo, A.; Tempczyk, A.; Grzonka, Z. *J. Comput.-Aided Mol. Design* **1989**, *3*, 261.

(56) Stein, S. E.; Barton, B. D. *Thermochim. Acta* **1981**, *44*, 265.

(57) Lubkowski, J.; Blazejowski, J. *J. Chem. Soc., Faraday Trans. 1* **1986**, *82*, 3069.

(58) Lias, S. G.; Liebman, J. F.; Levin, R. D. *J. Phys. Chem. Ref. Data* **1984**, *13*, 695.

(59) Willis, J. B. *Trans. Faraday Soc.* **1947**, *43*, 97.

(60) Bergmann, E.; Engel, L.; Meyer, H. *Chem. Ber.* **1932**, *65*, 446.

(61) Cumper, C. W. N.; Grinman, R. F. A.; Vogel, A. I. *J. Chem. Soc.* **1962**, 4518.

(62) Galy, A.-M.; Galy, J. P.; Faure, R.; Barbe, J. *Eur. J. Med. Chem. Chim. Theor.* **1980**, *15*, 179.

(63) Lutskii, A. E.; Prezhdo, V. V. *Zh. Fiz. Khim.* **1971**, *45*, 1273.

(64) Dauter, Z.; Bogucka-Ledochowska, M.; Hempel, M.; Ledochowski, A.; Kosturkiewicz, Z. *Rocz. Chem.* **1975**, *49*, 859; **1976**, *50*, 1573.

Table III. Energy Barriers for Structural Transformations (kcal/mol)[a]

compd	rotation around C_9–N_{23}	inversion at N_{23}	inversion of the whole molecule
11	4.973	0.100	
12			0.298
13	15.750		
14	0.115		
15			2.387
16	0.128		
17			1.618

[a] For structures of molecules at the saddle point see Figure 4 in supplementary material.

N_{23}, and two hydrogens at N_{10} are situated in one plane which is also the plane of symmetry of the molecule.

The $=NH$ and $=NH_2^+$ groups in imino structures **12**, **15**, and **17** lie almost in the plane created by the neighboring fragment of acridine (Table II). The boundary case is the lowest energy structure of monoprotonated 9-AA **14** in which all the atoms lie in one plane. The $-NH_3^+$ group in **14** and **16**, as well as the $-NH_2$ group in **11**, are located symmetrically relative to the plane of symmetry perpendicular to the skeleton of these molecules, although the C_9NH_2 fragment in **11** forms a deformed pyramid.

The change from amino to imino tautomer always accompanies shortening of the C_9–N_{23} and lengthening of the N_{10}–C_{12} bond (Table II). Accordingly, increase and decrease of the bond orders is predicted. This conforms with expected loss of aromacity by the central ring system and increase of the double-bond character of the C_9–N_{23} bond.

To learn how far structures obtained by AM1 geometry optimization correspond to those determined by X-ray analysis, we compared **Z** matrices for neutral 9-AA, existing in 9-acridinamine hemihydrate[32] (Table IV in supplementary material), and the monoprotonated molecule, occurring the monohydrate[33] and dihydrate of chloride salt (Table V in supplementary material), as well as net acridine[65] and the molecule bound in bis(acridine)pyromellitic dianhydride.[66] In regard to the acridine skeleton, both theoretical and crystallographic data reveal its planarity, although the bonds are predicted to be slightly longer in the gaseous phase. Valence and dihedral angles correspond quite well to each other except for those determining the location of hydrogen atoms at the exocyclic nitrogen. The $-NH_2$ group in 9-AA is more planar in the solid than gaseous phase. For the monoprotonated molecule the AM1 method predicts a completely planar structure of the $-NH_2$ fragment, whereas in both salts it is more or less pyramidal and slightly twisted against the acridine moiety.

Structural Transformations. The tautomers of neutral, mono-, and doubly protonated 9-AA may undergo structural transformations, those worth considering being rotation around C_9–N_{23}, inversion at N_{23}, and whole molecules. The energy barrier of ca. 5 kcal/mol (Table III) must be overcome for rotation of the $-NH_2$ group in neutral 9-AA. In the transition state this group is perpendicular to the acridine skeleton. Moreover, the transfer is accompanied by a change in the C_9–N_{23}–H_{24}–H_{25} angle from 147.7 to 121.3°, which means that the $-NH_2$ group is more planar in the lowest energy structure than in the transition state. Rotation in **13** proceeds through the transition state in which the $-NH_2$ fragment is also perpendicular to the acridine. This seems unlikely, however, owing to the relatively high energy barrier. The very low barriers in **14** and **16** occur whenever any N_{23}–H bond of the $-NH_3^+$ group crosses the plane created by the acridine moiety. In the latter case, the rotating group has to overcome only steric hindrances which, as calculations show, are negligible. On the other hand, rotation of $-NH_2$ in **11** and **13** is accompanied by the loss of conjugation between the lone electron pair at N_{23} and the acridine aromatic system. The rotation barrier can thus be considered to be a measure of this effect.

Inversion at N_{23} in the amino tautomer of neutral 9-AA requires the overcoming of an energy barrier of only 0.100 kcal/mol (Table III). The molecule in the transition state is completely planar. The energy barriers for the inversion of NH_3, c-$C_6H_{11}NH_2$, and $[(CH_3)_3C]_3N$, as AM1 predicts, are (in kcal/mol) as follows: 4.240, 2.893, and 2.285, respectively. This lowering of the energy barrier when moving from NH_3 and aliphatic amines to aromatic 9-AA is, therefore, due to conjugation of the ring rather than steric effects.

Inversion of the non-planar imino structures (**12**, **15**, and **17**) to their mirror images requires a planar acridine ring system at the saddle point. The relatively low energy barriers in this case (Table III) may cause transformation of molecules in room temperature.

Physicochemical Characteristics. The predicted values of ΔH_f are higher than determined experimentally (Table I). It is rather difficult to account for these discrepancies, although it is well-know that calorimetric methods do not always provide reliable thermochemical data when applied to compounds containing nitrogen atoms.

The enthalpies of formation of neutral molecules (B) and corresponding protonated forms (BH^+) enable the evaluation of proton affinities (PA), i.e., enthalpy changes for the process:[57,58,67]

$$BH^+ \rightarrow B + H^+ \qquad (2)$$

As the AM1 method reproduces the heat of formation of the proton rather poorly,[67] we applied the experimental value of $\Delta H_{f,g}{}^\circ[H^+]$ (equal to 367.2 kcal/mol[67]). When the first proton is attached to 9-AA, it is a stronger base than acridine (Table I). Both compounds are also much stronger bases than ammonia (for which the PA value derived by AM1 is equal to 209.3 kcal/mol; experimental = 205.5 kcal/mol[68]). The basicity of singly protonated 9-AA drops markedly as compared with that of the neutral molecule. This explains experimental observations that 9-acridinamine can be converted to the doubly protonated form only in strongly acidic media.[10,15]

The dipole moment (DM) predicted for acridine has a lower value than that reported in the literature (Table I), although correlation can be considered quite good. For 9-AA the AM1 method predicts much lower values than estimated experimentally. The possible explanation of this discrepancy may be that in the liquid phase solvation effects enhance charge separation in the molecules. It can also be noticed that dipole moments of amino and imino tautomers do not differ markedly. One could not, therefore, expect that this quantity would be helpful in studying tautomeric phenomena in 9-AA. From this point of view, earlier works whose authors predicted much lower values of DM for the imino than for the amino form and concluded that the relatively high experimental value of DM of 9-AA results from the existence of the molecule in the amino form only do not seem convincing.[7,21,26]

---

(65) Phillips, D. C.; Ahmed, F. R.; Barnes, W. H. *Acta Crystallogr.* **1960**, *13*, 365.

(66) Karl, N.; Binder, W.; Kollat, P.; Stezowski, J. J. *Acta Crystallogr., Sect. B* **1982**, *38*, 2919.

(67) Dewar, M. J. S.; Dieter, K. M. *J. Am. Chem. Soc.* **1986**, *108*, 8075.

(68) Jenkins, H. D. B.; Morris, D. F. C. *J. Chem. Soc., Faraday Trans. 2* **1984**, *80*, 1167.

The existence of dipole moments for acridine and 9-AA indicates nonuniform distribution of a charge (net atomic charges are given in Table VI of supplementary material). For both neutral and charged species AM1 usually predicts deficiency of a negative charge on hydrogen atoms and excess charge on carbon and particularly on nitrogen atoms. The charge is, therefore, distributed according to the electronegativity of atoms. These results do not conform with our traditional beliefs, particularly in the case of protonated species, which habitually assume that deficiency of a charge occurs on the nitrogen atom to which the proton is attached. According to the theoretical predictions the carbon and nitrogen atoms form a negatively charged core surrounded by a positively charged layer holding hydrogen atoms. Similar features have been predicted for other protonated nitrogen organic bases.[69]

According to Koopman's theorem[70] the energies (E) of the lowest unoccupied (LUMO) and highest occupied (HOMO) molecular orbitals, multiplied by -1, can be considered, in the first approximation, as electron affinity (EA) and ionization potential (IP) of a molecule, respectively.[71,72] In reality both latter quantities fulfil the linear relationship given by eq 3[73] in which δ is the *reorganization*

$$\mathrm{EA(IP)} = -E_{\mathrm{LUMO}}(E_{\mathrm{HOMO}}) - \delta_{\mathrm{LUMO}}(\delta_{\mathrm{HOMO}}) \qquad (3)$$

energy correction and results from the fact that all the electrons of the molecule undergo relaxation upon addition (or subtraction) of an electron. The negative values of E_{LUMO} and E_{HOMO} (Table I) can be compared with the electron affinity and ionization potential (in eV), respectively, only in the case of acridine (literature EA values are 0.75,[73] 0.88,[74] and 0.92;[75] IP values are 7.9[76] and 9.54[77]). The literature values correspond reasonably well to those calculated by AM1. To our knowledge no information regarding EA and IP is available for 9-AA.

The energies of LUMO and HOMO can further be related to the reductive and oxidative capability of the molecules.[75,78] Thus, the lower the HOMO (higher ionization potential) energy, the higher its resistance to oxidation. The measure of this latter feature may be the half-wave potential which for acridine (in V, equal to 1.35,[79] 1.36,[80] and 1.54[19]) and 9-AA (equal to 0.87 V[19]) follow the tendency of changes of E_{HOMO} (Table I). To consider the ability of molecules to undergo reduction it is worth remembering that the lower the energy of LUMO (higher electron affinity) the higher the tendency to undergo reduction (lower value of half-wave reduction potential). In this case, therefore, both quantities should be inversely related. This is roughly observed comparing the half-wave reduction potential, in V, of neutral acridine (-1.09,[81] -1.22,[18] -1.53,[20] -1.57,[78] -1.62,[75] and -1.68[82]) and 9-AA (-1.38,[81] -1.52,[18] and -1.78[20]), as well as protonated forms of the compounds (-0.44 for acridine[18,81] and -0.98 and -1.09 for 9-AA[18,81]), with energies of LUMO's listed in Table I, despite the fact that the experimental values are greatly scattered. It is also worth noting that the decrease in values of reduction potentials for protonated acridine and 9-AA, in relation to those of neutral molecules, is accompanied by a substantial increase in the electron affinity of the charged species.

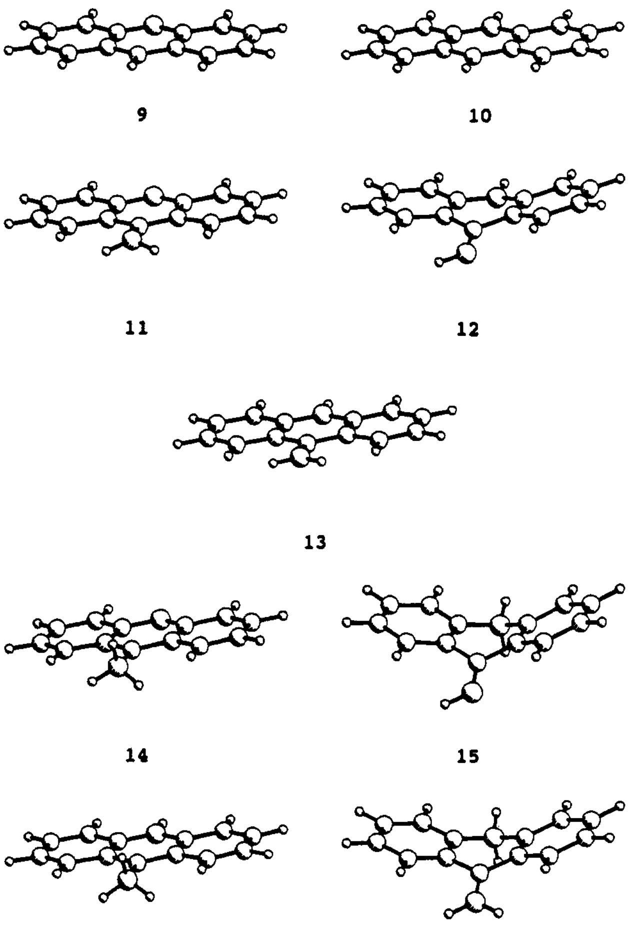

Figure 1. Lowest energy structures of neutral (**9**) and protonated (**10**) acridine; 9-acridinamine in amino (**11**) and imino (**12**) tautomeric forms; monoprotonated 9-acridinamine in mesomeric amino–imino (**13**), amino (**14**), and imino (**15**) forms; and doubly protonated 9-acridinamine in amino (**16**) and imino (**17**) forms.

Electrostatic Potential around Molecules. Two zones of potential appear around all neutral molecules (Figures 2 and 3). The region of the negative potential is in the neighborhood of the endocyclic nitrogen, in the acridine and amino tautomer of 9-AA, or around the exocyclic nitrogen in the amino tautomer of 9-AA. This implies that transfer of the hydrogen atom, following the change from amino to imino structure, is accompanied by the migration of electric poles in the opposite direction and thus inversion in the direction of the dipole moment. The zone of a positive potential surrounds the major part of the acridine moiety of the neutral molecules including the $-NH_2$ group, in the amino tautomer of 9-AA, and endocyclic nitrogen in the imino tautomer.

In both tautomers of 9-AA a relatively high gradient of electrostatic potential exists around endocyclic and exocyclic nitrogens. Such regions may primarily be considered as sites of specific interactions.[42] These include first and foremost, solute–solvent interactions, as well as those leading to the formation of associates (e.g., dimers).

---

(69) Lubkowski, J.; Blazejowski, J. *J. Phys. Chem.* **1991**, *95*, 2311.
(70) Koopmans, T. *Physica* **1934**, *1*, 104.
(71) Hush, N. S.; Pople, J. A. *Trans. Faraday Soc.* **1955**, *51*, 600.
(72) Roothaan, C. C. J. *Rev. Mod. Phys.* **1951**, *23*, 61.
(73) Younkin, J. M.; Smith, L. J.; Compton, R. N. *Theor. Chim. Acta* **1976**, *41*, 157.
(74) Dillow, G. W.; Kebarle, P. *Can. J. Chem.* **1989**, *67*, 1628.
(75) Tabner, B. J.; Yandle, J. R. *J. Chem. Soc.* **1968**, 381.
(76) El-Bayoumi, M. A.; Khalil, O. S. *J. Chem. Phys.* **1967**, *47*, 4863.
(77) Ciureanu, M.; Sahini, V. E. *Rev. Roum. Chim.* **1975**, *20*, 1037.
(78) Podany, V.; Vachalkova, A.; Miertus, S.; Bahna, L. *Neoplasma* **1975**, *22*, 469.
(79) Yasukouchi, K.; Taniguchi, I.; Yamaguchi, H.; Arakawa, K. *J. Electroanal. Chem. Interfacial Electrochem.* **1981**, *121*, 231.
(80) Vibopuu, H.; Vodzinskii, Yu. V.; Tikhova, N. Yu.; Kirso, U.; Jacquignon, P. S. *Zh. Obshch. Khim.* **1987**, *57*, 1379.
(81) Chodkowski, J.; Chrzanowski, A. *Rocz. Chem.* **1976**, *50*, 935.
(82) Maruyama, M.; Murukami, K. *J. Electroanal. Chem.* **1979**, *102*, 221.

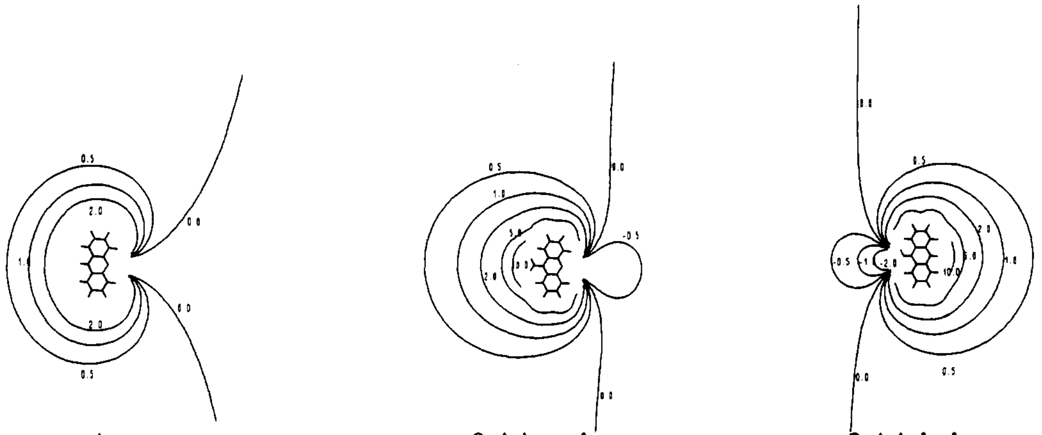

Acr 9-AA-amino 9-AA-imino

Figure 2. Two-dimensional (2-D) maps of the molecular electrostatic potential.

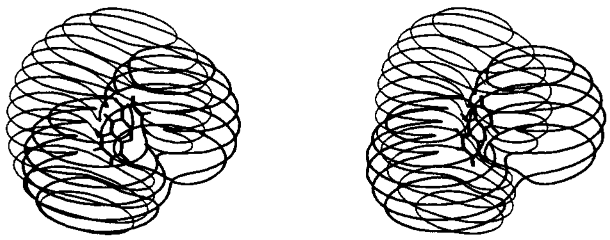

Acr

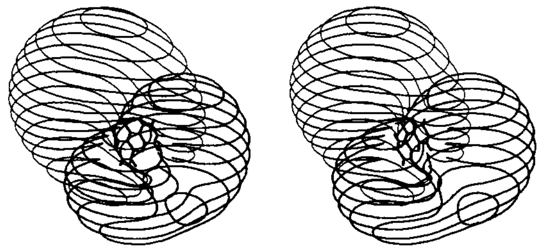

9-AA-amino

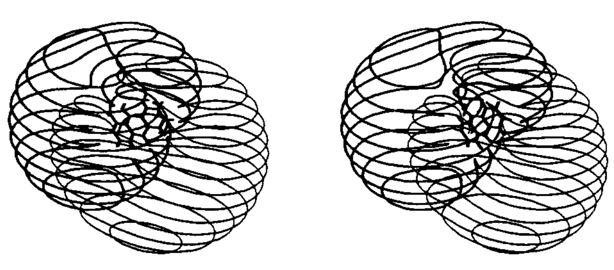

9-AA-imino

Figure 3. Stereoviews of the three-dimensional (3-D) maps of the molecular electrostatic potential.

Furthermore, these features may play a role in molecular recognition, as well as interactions with receptors and other macromolecules in living organisms. Knowledge of the distribution of the electrostatic potential around 9-AA should shed some light on the nature of the biological activity of the molecule.

All protonated molecules create a positive potential around themselves which resembles a single point charge potential on increasing the distance from the molecule. From the point of view of molecular interactions such species will tend to interact with negative poles of other molecules without engaging their own specific sites.

Conclusions

The problem of the true constitution of 9-acridinamine has attracted the attention of scientists since the beginning of the century. It is perhaps worth mentioning that in the second edition of Beilstein the compound is given under the imino structure. The problem was also the subject of intensive investigations as from the 1950's, but some questions remained unsolved. We believe that this work supplies the answer to at least some of them.

The theoretical calculations reveal that the 9-AA and its doubly protonated form exist, at room temperature, in two tautomeric forms. The equilibrium constants derived using data from Table I are as follows: 0.32 (for the equilibrium $11 \rightleftharpoons 12$) and 0.76 (for the equilibrium $16 \rightleftharpoons 17$). In both above cases the entropy changes are negative and the entropy factor has a significant influence on the state of equilibrium. Singly protonated 9-AA most probably exists in one structural form (**13**) only as other possible structures are not thermodynamically favored.

To be more certain of the finding discussed, other evidence would be welcome. For these reasons we have studied the electronic absorption spectra, both experimentally and theoretically.[83] We are also currently applying time-resolved and stationary fluorescence techniques to examine the problem. The information already gathered seems to confirm the results.

Acknowledgment. We would like to thank Dr. A. Liwo for permitting us to use the program for calculations and drawing the molecular electrostatic potential maps. This work was supported by the Polish State Committee for Scientific Research (KBN) under grant DS/5-300-7-016-1.

Registry No. **9**, 260-94-6; **10**, 22559-71-3; **11**, 90-45-9; **12**, 110166-26-2; **13**, 53502-36-6; **14**, 39041-79-7; **16**, 56402-31-4; **17**, 141292-11-7; H$^+$, 12408-02-5.

Supplementary Material Available: Tables IV and V in which Z matrices of neutral and monoprotonated 9-acridinamine resulting from AM1 optimization are compared with those obtained from crystallographic information, Table VI in which net atomic charges of all molecules shown in Figure 1 are compiled, and Figure 4 which presents transition state structures for structural transformations (6 pages). Ordering information is given on any current masthead page.

---

[83] Rak, J.; Blazejowski, J. *J. Photochem. Photobiol. A*, in press.